Acta Crystallographica Section F
Structural Biology and Crystallization Communications
ISSN 1744-3091

Expression, purification, crystallization and preliminary X-ray analysis of the human NORE1 SARAH domain

Hye Jin Kim,[a,b] Eunha Hwang,[a,c] Young-Hyun Han,[a] Saehae Choi,[a] Woo Cheol Lee,[a] Hye-Yeon Kim,[a] Young Ho Jeon,[d] Chaejoon Cheong[a,b] and Hae-Kap Cheong[a]*

[a]Division of Magnetic Resonance, Korea Basic Science Institute, 162 Yeongudanji-Ro, Ochang, Chungbuk 363-883, Republic of Korea, [b]Department of Bio-Analytical Science, Korea University of Science and Technology, Daejeon 305-350, Republic of Korea, [c]Division of Biotechnology, College of Life Science and Biotechnology, Korea University, Seoul 136-701, Republic of Korea, and [d]College of Pharmacy, Korea University, Jochiwon, Chungnam 339-700, Republic of Korea

Correspondence e-mail: haekap@kbsi.re.kr

Received 3 April 2012
Accepted 14 May 2012

NORE1 is an important tumour suppressor in human cancers that interacts with the pro-apoptotic protein kinase MST1/2 through SARAH domains. The SARAH domain (residues 366–413) of human NORE1 was expressed in *Escherichia coli*, purified and crystallized using the hanging-drop vapour-diffusion method. The crystal diffracted to 2.7 Å resolution and belonged to space group $P6_122$, with unit-cell parameters $a = b = 73.041$, $c = 66.092$ Å, $\alpha = \beta = 90$, $\gamma = 120^\circ$.

1. Introduction

Ras is a small GTPase that functions as a GDP/GTP binary molecular switch at the inner-cell surface of the plasma membrane in response to extracellular ligand signals such as growth factors, cytokines, hormones and neurotransmitters (Campbell *et al.*, 1998). GTP-bound Ras modulates multiple signalling pathways that regulate cell proliferation, differentiation and apoptosis through the binding of different Ras effectors (Feig & Buchsbaum, 2002). Rassf (Ras association domain family) proteins are Ras effectors that interact with the active form of Ras in a variety of human cancers (Agathanggelou *et al.*, 2005). NORE1 (novel Ras effector 1; also termed Rassf5 or RAPL) has been identified as a Ras effector protein that directly interacts with active GTP-bound Ras and promotes apoptosis (Vavvas *et al.*, 1998). NORE1 and Rassf1 are the best-characterized proteins in the Rassf family and share high sequence homology (∼50%; Aoyama *et al.*, 2004; Avruch *et al.*, 2009). NORE1 contains three domains: a cysteine-rich zinc finger (C1), a Ras-binding domain (RBD) and a protein–protein interaction motif (SARAH). The C1 domain forms an intramolecular complex with the RBD that is disrupted by RBD binding to GTP-bound Ras (Harjes *et al.*, 2006). SARAH domains have a predicted coiled-coil structure and consist of approximately 50 conserved residues found in the C-terminal regions of Salvador, Rassf and Hippo proteins (Scheel & Hofmann, 2003). The NORE1 SARAH domain interacts with the pro-apoptotic protein kinase mammalian sterile 20-like kinase 1/2 (MST1/2) as a heterodimer *via* its SARAH domain and promotes apoptosis and cell-cycle arrest (Hwang *et al.*, 2007; Khokhlatchev *et al.*, 2002). This heterodimeric interaction has been implicated in Ras-mediated apoptotic signalling (Scheel & Hofmann, 2003).

A previous structural study of the MST1 SARAH domain showed it to be an antiparallel, helical, homodimeric structure which interacts with the SARAH domains of NORE1 and WW45 (Hwang *et al.*, 2007). Structural studies of the NORE1 SARAH domain may illuminate the Ras–Rassf–MST1/2 pathway and increase our understanding of its role in apoptosis. Here, we report the cloning, purification, crystallization and preliminary X-ray analysis of the human NORE1 SARAH domain.

2. Materials and methods

2.1. Cloning

The NORE1 SARAH domain (residues 366–413) was amplified by PCR from the NORE1 cDNA (GenBank accession No. NP872604)

using the forward primer 5′-CGC**GGATCC**GAGGTAGAGTGG-GATGCC-3′ and the reverse primer 5′-GGC**CTCGAG**TTACCCA-GGTTTGCCCTG-3′. The PCR products were digested with the restriction enzymes *Bam*HI and *Xho*I and inserted into the *Bam*HI/*Xho*I restriction-enzyme sites of the pGEX4T-1 vector (GE Healthcare, USA). The plasmid sequence was verified by a commercial DNA-sequencing service (Solgent, Republic of Korea). Plasmids harbouring the NORE1 SARAH domain were transformed into *Escherichia coli* strain BL21.

2.2. Protein expression and purification

Transformed colonies were cultured in LB medium containing 100 µg ml^{-1} ampicillin at 310 K until an OD_{600} of 0.5–0.6 was reached. Expression of recombinant NORE1 SARAH domain was induced with 0.5 m*M* isopropyl *β*-D-1-thiogalactopyranoside (IPTG) and the incubation temperature was decreased to 291 K. After growth for 16 h, the cells were harvested by centrifugation at 6000*g* for 20 min and the cell pellets were resuspended in lysis buffer (20 m*M* Tris–HCl pH 7.0, 500 m*M* NaCl, 10% glycerol, 2 m*M* DTT) containing 1 m*M* benzamidine, 1 m*M* bacitracin and 1 m*M* phenylmethylsulfonyl fluoride (PMSF). After the resuspended cells had been incubated for 20 min on ice, the cells were sonicated (using a tip sonicator whilst on ice) and the supernatant was separated from the pellet by centrifugation at 18 000*g* for 40 min at 277 K. The supernatant was loaded onto a 5 ml GST FF column (GE Healthcare) pre-equilibrated with binding buffer (PBS pH 7.4, 100 m*M* NaCl, 2 m*M* DTT) and washed with five column volumes of binding buffer. GST-fused NORE1 SARAH domain was eluted with elution buffer (50 m*M* Tris–HCl pH 8.0, 100 m*M* NaCl, 10 m*M* glutathione). The eluted protein was cleaved with thrombin overnight at 293 K (Haematologic Technologies) to remove the GST tag and was concentrated to 1 ml using an Amicon Ultra-15 filter (Millipore). Finally, the protein was purified using HiLoad Superdex 75 16/60 (GE Healthcare) in a buffer consisting of 25 m*M* HEPES pH 7.0, 100 m*M* NaCl, 2 m*M* DTT. The homogeneity of the purified 6.3 kDa protein was confirmed by 18% SDS–PAGE (Fig. 1). The fractions containing the NORE1 SARAH domain were collected and concentrated to 13.8 mg ml^{-1} using an Amicon Ultra-15 filter (Millipore). The protein concentration was determined by the Bradford assay method (Bradford, 1976).

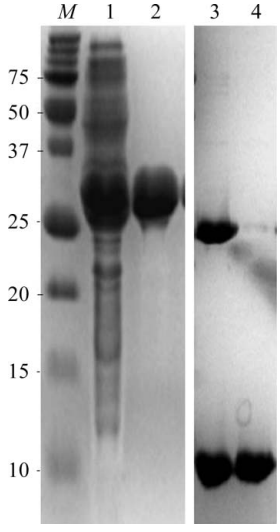

Figure 1
SDS–PAGE analysis of the NORE1 SARAH domain during purification. Lane *M*, molecular-weight marker (labelled in kDa); lane 1, *E. coli* extract expressing GST-NORE1 SARAH domain; lane 2, proteins from a GST affinity column; lane 3, GST tag and NORE1 SARAH domain bands after thrombin cleavage (upper and lower bands, respectively); lane 4, proteins separated after Superdex 75 chromatography.

2.3. Crystallization

Screening of crystallization conditions for the NORE1 SARAH domain was performed with 384 conditions from screening kits including Wizard I and II (Emerald BioSystems), Crystal Screen, Crystal Screen 2, PEG/Ion and SaltRx (Hampton Research) using the sitting-drop vapour-diffusion method. Each screen solution was mixed with protein solution, dispensed onto a 96-well Intelli-Plate (Hampton Research) using a Mosquito nanolitre liquid-dispensing robot (TTP Labtech) and incubated at 293 K. The reservoir volume was 70 µl and the drop consisted of 0.4 µl protein solution and 0.4 µl reservoir solution. Crystals appeared within a week in Wizard condition No. 14 from the initial screen. The crystals were manually reproduced and optimized using the 96-condition Additive Screen (Hampton Research). Protein solution (1 µl) was mixed with additive solution (0.2 µl) and reservoir solution (1 µl) and equilibrated against reservoir solution (500 µl) in a VDX plate (Hampton Research) using the hanging-drop vapour-diffusion method.

2.4. Data collection and processing

The crystals were soaked in a cryoprotectant solution consisting of 30%(*v*/*v*) glycerol or 14%(*v*/*v*) sucrose and flash-cooled in a nitrogen stream at 100 K. X-ray diffraction data were collected from the cooled crystals using an ADSC Quantum 210 CCD detector on beamline 6C at Pohang Accelerator Laboratory (PAL; Pohang, Republic of Korea). A total of 120 data frames were measured with an oscillation angle of 1.0°. The wavelength of the X-ray beam was 1.23985 Å and the crystal-to-detector distance was 180 mm. Data were integrated and scaled using the *HKL*-2000 software suite (Otwinowski & Minor, 1997).

3. Results and discussion

The NORE1 SARAH domain was expressed in *E. coli* and purified using GSH Sepharose columns and gel filtration. We were able to obtain ∼10 mg purified protein per 1 l culture. The purified protein was concentrated to 13.8 mg ml^{-1} and used to screen for crystallization conditions. Eventually, we obtained crystals using a solution consisting of 1.2 *M* sodium citrate, 0.1 *M* sodium cacodylate pH 6.5,

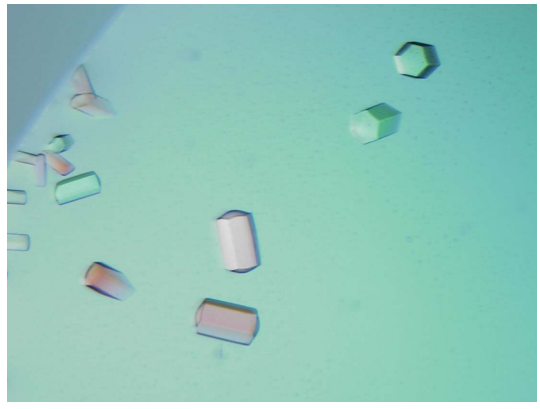

Figure 2
Crystals of the NORE1 SARAH domain. The crystals were grown in the presence of 1.2 *M* sodium citrate, 0.1 *M* sodium cacodylate pH 6.5 and 0.5% octyl *β*-D-glucopyranoside at 293 K. The approximate dimensions of the crystals were 0.1 × 0.2 × 0.1 mm.

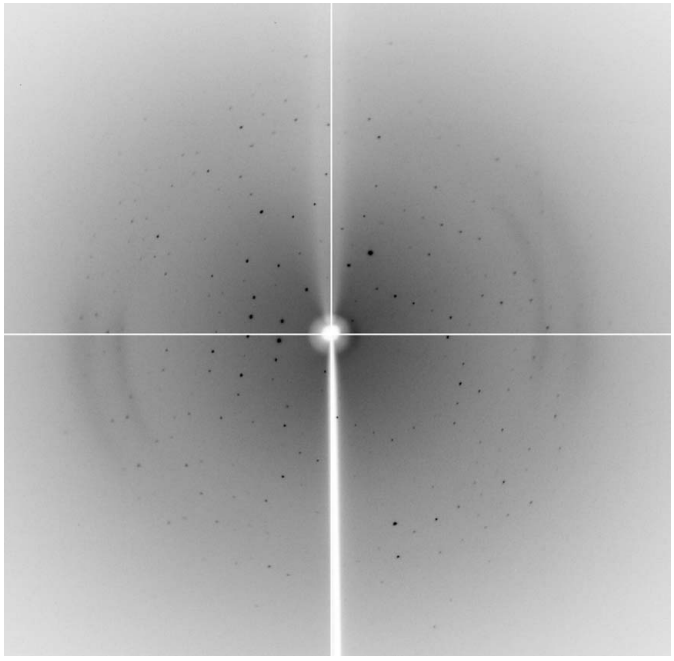

Figure 3
X-ray diffraction image obtained from a crystal of the NORE1 SARAH domain. The edge of the detector corresponds to a resolution of 2.7 Å.

0.5% octyl β-D-glucopyranoside at 293 K. Single crystals of the NORE1 SARAH domain usually grew within 1–2 weeks and were suitable for X-ray diffraction experiments (Fig. 2). The native crystal of the NORE1 SARAH domain diffracted to 2.7 Å resolution and belonged to a primitive hexagonal unit cell, with unit-cell parameters $a = b = 73.041$, $c = 66.092$ Å, $\alpha = \beta = 90$, $\gamma = 120^\circ$ (Fig. 3). Data-collection statistics are given in Table 1. Based on the scaled data, the extinction of *l*-axis reflections except for those with $l = 6n$ indicated a hexagonal lattice and space group $P6_122$ was assigned using the program *POINTLESS* (Evans, 2007). This space group gave a calculated Matthews coefficient (V_M) of 2.26 Å^3 Da^{-1} and a solvent content of 45%; there were two molecules in the asymmetric unit (Matthews, 1968). We attempted molecular replacement with the program *Phaser* (McCoy *et al.*, 2005) using the structure of the MST1 SARAH domain (PDB entry 2jo8; Hwang *et al.*, 2007) as a model. However, no solution could be found.

Rassf1 and NORE1 can form both homodimers and heterodimers (Ortiz-Vega *et al.*, 2002). Therefore, we assumed that the NORE1 SARAH domain forms a homodimer. The solution structure of the MST1 SARAH domain shows a slightly distorted α-helix owing to the presence of two proline residues (Hwang *et al.*, 2007). The sequence identity between the NORE1 SARAH domain (residues 361–413) and the MST1 SARAH domain (residues 433–482) is 25%, but these proline residues are absent in the NORE1 SARAH domain. It is most likely that the structure will be a straight anti-parallel α-helix.

In a previous study, the MST1 SARAH domain and the NORE1 SARAH domain formed a heterodimer (Hwang *et al.*, 2007). These preliminary X-ray data will be useful for further understanding of the apoptotic pathways mediated by the homodimeric and heterodimeric structures of Rassf proteins and MST1/2 formed *via* their SARAH domains. Crystal structure determination is currently under way using the multi-wavelength anomalous dispersion method with selenium as an anomalous scatterer (Terwilliger, 1994).

Table 1
X-ray data-collection statistics.

Values in parentheses are for the highest resolution shell.

Beamline	6C, PAL
Temperature (K)	100
Oscillation range (°)	1
Space group	$P6_122$
Unit-cell parameters (Å, °)	$a = 73.060$, $b = 73.060$, $c = 66.042$, $\alpha = 90$, $\beta = 90$, $\gamma = 120$
Resolution range (Å)	50–2.70 (2.75–2.70)
Unique reflections	141480
Matthews coefficient (Å^3 Da^{-1})	2.26
Molecules in asymmetric unit	2
Multiplicity	8.0 (4.4)
Completeness (%)	98.2 (98.1)
R_{merge}† (%)	0.055 (0.321)
Mean $I/\sigma(I)$	14.0 (2.5)

† $R_{merge} = \sum_{hkl}\sum_i |I_i(hkl) - \langle I(hkl)\rangle| / \sum_{hkl}\sum_i I_i(hkl)$.

This work was supported by funding from the High Field NMR Research Program of the Korea Basic Science Institute. We thank the staff of beamline 6C at Pohang Accelerator Laboratory for help with X-ray data collection.

References

Agathanggelou, A., Cooper, W. N. & Latif, F. (2005). *Cancer Res.* **65**, 3497–3508.
Aoyama, Y., Avruch, J. & Zhang, X.-F. (2004). *Oncogene*, **23**, 3426–3433.
Avruch, J., Xavier, R., Bardeesy, N., Zhang, X.-F., Praskova, M., Zhou, D. & Xia, F. (2009). *J. Biol. Chem.* **284**, 11001–11005.
Bradford, M. M. (1976). *Anal. Biochem.* **72**, 248–254.
Campbell, S. L., Khosravi-Far, R., Rossman, K. L., Clark, G. J. & Der, C. J. (1998). *Oncogene*, **17**, 1395–1413.
Evans, P. R. (2007). *Acta Cryst.* D**63**, 58–61.
Feig, L. A. & Buchsbaum, R. J. (2002). *Curr. Biol.* **12**, R259–R261.
Harjes, E., Harjes, S., Wohlgemuth, S., Müller, K.-H., Krieger, E., Herrmann, C. & Bayer, P. (2006). *Structure*, **14**, 881–888.
Hwang, E., Ryu, K.-S., Pääkkönen, K., Güntert, P., Cheong, H.-K., Lim, D.-S., Lee, J.-O., Jeon, Y. H. & Cheong, C. (2007). *Proc. Natl Acad. Sci. USA*, **104**, 9236–9241.
Khokhlatchev, A., Rabizadeh, S., Xavier, R., Nedwidek, M., Chen, T., Zhang, X.-F., Seed, B. & Avruch, J. (2002). *Curr. Biol.* **12**, 253–265.
Matthews, B. W. (1968). *J. Mol. Biol.* **33**, 491–497.
McCoy, A. J., Grosse-Kunstleve, R. W., Storoni, L. C. & Read, R. J. (2005). *Acta Cryst.* D**61**, 458–464.
Ortiz-Vega, S., Khokhlatchev, A., Nedwidek, M., Zhang, X.-F., Dammann, R., Pfeifer, G. P. & Avruch, J. (2002). *Oncogene*, **21**, 1381–1390.
Otwinowski, Z. & Minor, W. (1997). *Methods Enzymol.* **276**, 307–326.
Scheel, H. & Hofmann, K. (2003). *Curr. Biol.* **13**, R899–R900.
Terwilliger, T. C. (1994). *Acta Cryst.* D**50**, 17–23.
Vavvas, D., Li, X., Avruch, J. & Zhang, X.-F. (1998). *J. Biol. Chem.* **273**, 5439–5442.